Steel and Composite Structures, *Vol. 36, No. 2 (2020) 163-177*
DOI: https://doi.org/10.12989/scs.2020.36.2.163

Performance of innovative composite buckling-restrained fuse for concentrically braced frames under cyclic loading

Masoud Mohammadi[1,2a], Mohammad A. Kafi[*1], Ali Kheyroddin[1b] and Hamid R. Ronagh[2c]

[1]*Department of Civil Engineering, Semnan University, Semnan, Iran*
[2]*Centre for Infrastructure Engineering, Western Sydney University, Penrith, Australia*

(*Received April 18, 2019, Revised June 26, 2020, Accepted July 6, 2020*)

Abstract. Concentrically Braced Frames (CBFs) are commonly used in the construction of steel structures because of their ease of implementation, rigidity, low lateral displacement, and cost-effectiveness. However, the principal disadvantage of this kind of braced frame is the inability to provide deformation capacity (ductility) and buckling of bracing elements before yielding. This paper aims to present a novel Composite Buckling Restrained Fuse (CBRF) to be utilized as a bracing segment in concentrically braced frames that allows higher ductility and removes premature buckling. The proposed CBRF with relatively small dimensions is an enhancement on the Reduced Length Buckling Restrained Braces (RL-BRBs), consists of steel core and additional tensile elements embedded in a concrete encasement. Employing tensile elements in this composite fuse with a new configuration enhances the energy dissipation efficiency and removes the tensile strength limitations that exist in bracing elements that contain RL-BRBs. Here, the optimal length of the CBRF is computed by considering the anticipated strain demand and the low-cyclic fatigue life of the core under standard loading protocol. An experimental program is conducted to explore the seismic behavior of the suggested CBRF compare with an RL-BRB specimen under gradually increased cyclic loading. Moreover, Hysteretic responses of the specimens are evaluated to calculate the design parameters such as energy dissipation potential, strength adjustment factors, and equivalent viscous damping. The findings show that the suggested fuse possess a ductile behavior with high energy absorption and sufficient resistance and a reasonably stable hysteresis response under compression and tension.

Keywords: steel structure; braced frame; energy dissipation; structural composite fuse; buckling restrained braces

1. Introduction

Lateral loads generated through earthquakes and wind are an important consideration in the design of structures. Engineers have long understood the need for lateral load resisting systems. One of the oldest framed structures which incorporated the very first lateral load resisting system is Chicago's Insurance Home, a 10-story building that was built in 1885 (Craighead 2009). The lateral load resisting systems were either braced systems or moment frames. Until the Northridge earthquake in 1994, moment frames were thought to resist earthquakes better as they were thought to be more ductile. In the Northridge earthquake, however, it was seen that steel moment frames with welded beam-to-column rigid connections were highly damaged (Engelhardt and Sabol 1995, Engelhardt and Sabol 1998). The damage sustained by moment frame structures were dispersed in the whole structure and thus were very costly to repair (EERI. 1995). Unlike moment frames, damages to concentrically braced frames were limited to the braces themselves and thus were less costly to repair. This generated a paradigm shift and resulted in many changes to the design standards (Bruneau *et al.* 2011). The only issue with the concentrically braced frames was that they were less ductile than moment frames. Many researches since have been concentrated on enhancing the ductility of CBF. The majority of these researches attempted to provide modifications in connections or embed a ductile member into concentric frames to raise the deformation capacity. Among these, Pall friction damper with frictional sliding surfaces (Pall and Marsh 1982), Popov friction connections (Grigorian *et al.* 1993), linear and rotational sliding friction connections (Mualla and Belev 2002), shear wall bracing as the original idea of Buckling-restrained braces (BRBs) by Yoshino and Karino (1971), test on braces encased by mortar in-filled steel tubes, composite buckling-restrained bracing placed in reinforced concrete components and modern buckling-restrained bracing with steel core, gaps with non-sticky materials and concrete encase (Fujimoto *et al.* 1988, Kim *et al.* 2004, Xie 2005, Mete Güneyisi *et al.* 2015, Maalek *et al.* 2019) can be named.

Among the energy dissipation devices, yielding elements as dampers and fuses can be used to increase the deformation capacity of braced systems. In 1980, primary examples of energy-absorbing steel elements were presented by Skinner to be used in buildings and bridges (Skinner *et al.* 1980). When these dampers are subjected to loads, they yield and dissipate large amounts of input energy of the structure. The

*Corresponding author, Associate Professor
E-mail: mkafi@semnan.ac.ir
[a]Ph. D.
[b]Professor
[c]Professor

ISSN: 1229-9367 (Print), 1598-6233 (Online)

existence of a fuse that yields at a certain load limits the damage to other elements of the system and avoids overload. Among these, triangular-shaped (TADAS, Triangular-plate Added Damping and Stiffness) and X-shaped (ADAS, Added Damping and Stiffness) dampers proposed by Tsai in 1993 that is able to highly absorb and sustain a considerable number of yieldings without any sign of strength or stiffness degradation (Tsai *et al.* 1993). Yielding central dampers by Jurukovski *et al.* (1995) as well as use of ring as a ductile and energy-absorbing element in concentrically braced frames can be mentioned (Gorji Azandariani *et al.* 2020a). Bazzaz *et al.* (2012, 2015a, b) examined the role of using half-ring elements in energy dissipation and sustaining hysteresis curves for Y-shaped bracing. Bonetti (2008) provided a composite fuse including rebar embedded in polymer matrix surrounded by FRP. Mirtaheri *et al.* (2011) modified BRBs with shorter lengths and used them as damper BRB in CBFs. Hoveidae *et al.* (2015) proposed short core buckling-restrained bracing analyzed its seismic behavior numerically and the effect of this system in reducing relative displacement of stories and substituting it with full core buckling brace. Pandikkadavath and Sahoo (2016b, 2017) presented the results of cyclic loading tests on Reduced-Length BRB (RL-BRB) with the aim of investigating the hysteretic behavior of these specimens as a bracing segment. This concept was further developed by Kachooee and Kafi (2018), and Mohammadi *et al.* (2019).

The present research attempts to represent a novel Composite Buckling Resistance Fuse (CBRF) to increase the ductility of concentrically braced frames and prevent early buckling of whole braces, allowing high energy dissipation and increasing the loading capacity to cope with lateral forces caused by earthquakes and other lateral loads. Despite the advantages of structural fuses (Jurukovski *et al.* 1995, Abdel Raheem and Hayashikawa 2013, Bergami and Nuti 2013, Calado *et al.* 2013, Karalis and Stylianidis 2013, Andalib *et al.* 2014, Dougka *et al.* 2014, Bazzaz *et al.* 2015b, Xu *et al.* 2016, Deihim and Kafi 2017, Andalib *et al.* 2018, Rashidi *et al.* 2018, Usefi *et al.* 2018, Bahirai and Gerami 2019, Gorji Azandariani *et al.* 2020b, Usefi *et al.* 2020) and also in continuation of previous works carried out by the researchers on RL-BRBs (Tremblay *et al.* 2004, Bonetti 2008, Fanaie and Dizaj 2014, Hoveidae *et al.* 2015, Dizaj *et al.* 2017, Mohammadi *et al.* 2017, Mohammadi *et al.* 2018a, Mohammadi *et al.* 2018b), this fuse is designed to be buckled and failed before the whole brace buckling in compression. Additional tensile elements have been utilized innovatively; therefore, no limitation of the tensile capacity of the whole brace can be occurred unlike what happens when a structural fuse or RL-BRB is utilized in a brace member. The small size of this CBRF makes it economical compared to that of full-length BRBs.

In the present research, the suggested buckling-restrained fuse is presented, and design details are discussed theoretically. The optimal core length is determined according to the anticipated core low-cyclic fatigue life and its strain demand. This study continued with an experimental evaluation of the hysteretic response of the CBRF compared with RL-BRB under cyclic loading. The experimental results on the proposed CBRF with extra tensile elements are described, its strength adjustment factors are investigated, and damping potential of the samples are quantified.

2. Main descriptions

Sacrificial elements or fuses are weak yielding elements which fail while absorbing considerable energy, thereby protecting the rest of the structure. In braced frames, the damage is often concentrated in the bracing members. When bracing members are equipped with fuses such as that suggested here, the anticipated damage in the bracing member will be focused in the fuse only. This further limits the damage. These fuses can be designed to improve ductility and damping characteristics of the structure as well. Fuses should be designed to yield at loads lower than the buckling load of the bracing member under compression or its yielding load under tension. Therefore, the buckling does not occur, and the bracing member does not fail prior to the fuse yielding.

The reduced-length BRB is a hysteretic fuse composed of steel parts restrained in a concrete encasement. This kind of short-length BRB is designed to be placed at the end of each bracing member. RL-BRB with almost similar tension and compression capacity can enter into the inelastic range to absorb energy while preventing global buckling of the primary bracing members (Razavi Tabatabaei *et al.* 2014, Pandikkadavath and Sahoo 2016b).

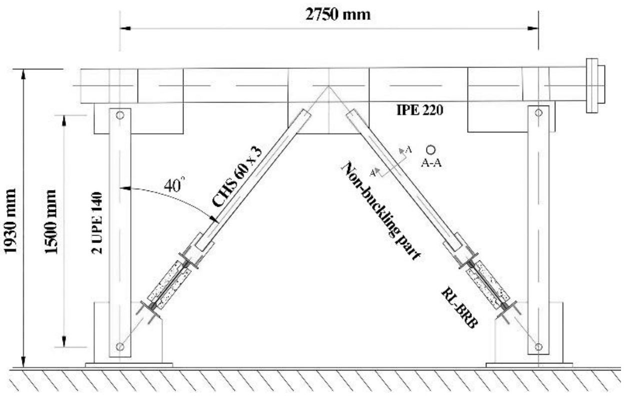

(a) RL-BRB in a chevron frame

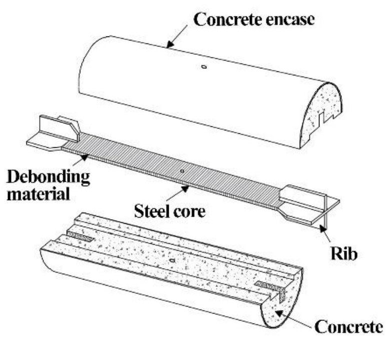

(b) RL-BRB components

Fig.1 Placement of RL-BRB and its components

An RL-BRB is easy to install, inspect and replaced cheaply after a serve loading such as an earthquake. Fig. 1(a), represents the placement of RL-BRB as a structural fuse in a concentrically braced frame. The RL-BRB comprises of four key parts including a central steel core, concrete encases, length and gap size between the core and encase which could be filled up with a soft material, Fig. 1(b). The proposed fuse in this research is an enhanced form of RL-BRB discussed in Section 3.

2.1 Central steel core of RL-BRB

Performance of an RL-BRB under compression and tension is different. The compressive load-bearing capacity of an RL-BRB depends on the cross-sectional area and on the type of the steel core. Steel bars or thin plates are the two possible candidates that can be designed considering a buckling strength modification factor over the main bracing element buckling capacity. The concrete encasement avoids the primary buckling of the central core in the first global buckling mode shape. The reason is that prior to this buckling, the core element buckles locally firstly in the first mode and gradually to the higher modes as it displaces axially. Originally while the loads are small, the core undergoes small axial shortening dictated by the strength of materials formula $\Delta = PL_c/EA$, in which Δ is defined as the core longitudinal displacement, P is the axial compressive force, EA is the core axial stiffness, and L_c is the length of the core. The average core strain is defined as $\varepsilon_{ca} = \Delta/L_c$. As the axial load increases the core buckles in its fundamental mode shapes. The contact between the core and the encasement as it locally buckles happens at the peaks of the sinusoidal local buckling waves. The peak contact points of the waves are the most likely area for development of the plastic hinges. The peak contact points provide forces need to be resisted by the encasement. In this regard, a theoretical study conducted by Jiang *et al.* (2017) comprehensively discussed the core buckling deformations of the BRBs.

Plastic behavior of the core material and formation of plastic hinges could enhance the energy dissipation for RL-BRB. Owing to the short length of RL-BRB, in the same relative displacement (Drift=Δ_x/H), the average core strain, ε_{ca}, would be more than the similar longer samples (BRBs). A typical application of Full-length BRB and RL-BRB are depicted in Fig. 2.

In order to have the desired performance for the RL-BRB under compressive loads, the core buckling has to occur in the inner part of the encasement, and outer parts of the core have to remain elastic without defect.

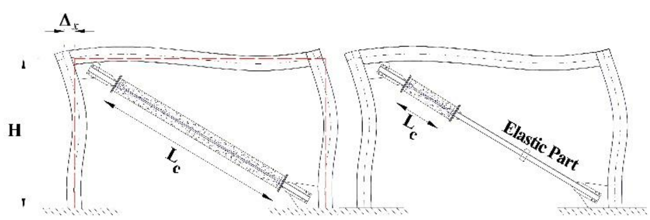

(a) full-length BRB (b) RL-BRB

Fig. 2 The application of RL-BRB and BRB in the frame

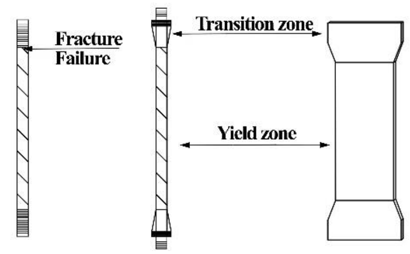

Fig. 3 Preliminary rod vs. samples of RL-BRB core

Fig. 3 demonstrates the considered transition zone with a larger cross-section than the inner yield zone for two kinds of the core. Different core types can be used for the RL-BRB. Steel thin plate (Razavi Tabatabaei *et al.* 2014) and steel bars (Bonetti 2008, Park *et al.* 2012) are two common types of the core used by researchers in the past. A steel core of circular section may buckle about any axis while a steel thin plate may only buckle about its minor axis. Therefore, use of thin plates for the core is a better option naturally as the direction of buckling is known and as such, it would be easier and more cost-effective to design an encasement that resists the contact forces of the buckled core at known positions. Double or triple thin core steel plate or some parallel steel bars with several layouts to improve the capacity of the segments in tension and compression have been employed (Hoveidae 2018).

2.2 Determination of the RL-BRB length

The fuse length, specifically the steel core length in RL-BRB, plays an important role in providing adequate ductility and absorbing sufficient energy in this system. Robert Tremblay *et al.* (2006) examined 6 BRB specimens with short lengths, and different encase. Their tests showed that BRBs with longer cores hardly entered the inelastic zone while shorter ones achieved higher strains easier at the same displacement (Tremblay *et al.* 2004, Robert Tremblay *et al.* 2006, Stratan *et al.* 2020, Zub *et al.* 2020). Therefore, when the core undergoes significant plastic deformation, the hysteretic energy dissipation will increase, though the sensitivity to low cyclic fatigue phenomena may increase. In order to arrive at an optimal length for the RL-BRB, two considerations were made. Firstly, the optimal length of the core with elastic material was obtained and secondly the minimum length of the core to prevent low-cycle fatigue was calculated as the core entered the plastic phase.

RL-BRB can be modeled elastically such as a linear spring located in the full-length brace, as shown in Fig. 4 (Hoveidae *et al.* 2015). Each part of the main brace is considered to work in the elastic phase too. Considering the Hooke's law, members with lower stiffness, K_i, would experience larger displacements under the same load as per Eq. (1).

$$\Delta_i \propto \frac{1}{K_i} = f_i \tag{1}$$

where Δ_i is the elastic displacement of the member i and K_i is stiffness of member i. Linear springs in series displace as per Eq. (2). Moreover, considering the elastic behavior and the threshold of yielding for the BRB core, and substituting for the material yield strain, ε_y, in Eq. (2), Eq. (3) can be obtained

$$\Delta_{Lb} = \Delta_{RL-BRB} + \Delta_{i-1} \tag{2}$$

$$\Delta_{Lb} = (\varepsilon_y \times L_c) + (\frac{P}{K_1} + \frac{P}{K_2} + ... + \frac{P}{K_i}) \tag{3}$$

in which Δ_{Lb} is the displacement of the whole brace that is dependent on the maximum story drift θ and shall not be taken less than 0.01 times the story height (AISC341 2016). Since the force, P, applied to each member must be similar to the yield force of the RL-BRB, we will have

$$L_c \leq \frac{\Delta_{Lb}}{\varepsilon_y \ (1 + K_c \sum(\frac{1}{K_i}))} \tag{4}$$

L_c and K_c represent respectively length of the core and linear stiffness of the CBRF core. Eq. (4) can be used to calculate the maximum length of the core, in accordance with the allowed story drift. To calculate the axial stiffness, K_i, of each member, Eq. (5) is used.

$$K_i = \frac{E_i}{\int_0^{L_i} \frac{dx}{A_i(x)}} \tag{5}$$

where E_i is the Elasticity Modulus, $A_i(x)$ represents the cross-sectional area as a function of distance, (x), and L_i is the length of the member i.

Material yielding of the core under the cyclic loads could exceed the probability of sudden and brittle low-cyclic fatigue (LCF) fracture for mechanical parts of the fuse. With Regard to the metallurgy, based on the adopted loading protocol and the number of inelastic cycles, N_f, we can evaluate the minimum length of the core to prevent LCF fracture by Coffin-Manson equation, Eq. (6), according to the total material strain (Budynas *et al.* 2011). Inelastic or plastic cycles are defined as the cycles during which the core was definitely entered into the plastic phase passing the yield deformation.

$$\frac{\Delta\varepsilon}{2} = \frac{\Delta\varepsilon_e}{2} + \frac{\Delta\varepsilon_p}{2} = \frac{\sigma_f}{E}(2N_f)^b + \varepsilon_f(2N_f)^c \tag{6}$$

where $\Delta\varepsilon$, $\Delta\varepsilon_e$, $\Delta\varepsilon_p$ are the total, elastic and plastic strain amplitudes respectively, σ_f and ε_f are fatigue strength and ductility; coefficient, b, and c are fatigue strength and ductility exponents and E is the Elasticity Modulus of the material. Since the elastic strain component is small in comparison to the plastic strain for the steel material, it can be neglected. As the loading protocol applied to the segment has a variable number of cycles at the same stress level, such as shown in Fig. 5, the damage sustained during multi-stage loading can be defined by the Palmgren-Miner cycle-ratio summation rule, Eq. (7) (Hashin and Rotem 1978, Budynas *et al.* 2011).

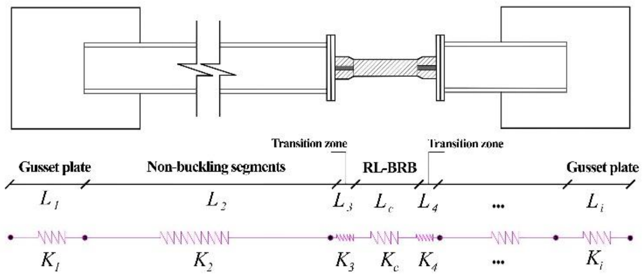

Fig. 4 Spring model of the brace with RL-BRB

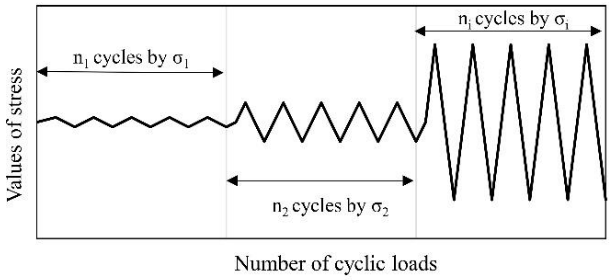

Fig. 5 Loading protocol sample

$$\sum \frac{n_i}{(N_f)_i} = D \tag{7}$$

where the n_i is the number of cycles at stress σ_i and N_f is the number of failure cycles at the level σ_i of stress.

The parameter D is usually determined by experiments, but it is also found with an average value near unity when the failure occurs so the minimum length of the core can be estimated when D falls below 1.0. Replacing Eq. (6) into the Eq. (7) yields

$$\sum_{i=1}^{m} \frac{n_i}{\frac{1}{2} \times (\frac{\Delta\varepsilon_i}{2 \times \varepsilon_f})^{\frac{1}{c}}} \leq 1 \tag{8}$$

where m is defined as the total number of the inelastic cycles acquired from the selected loading protocol and $\Delta\varepsilon_i$ is the value of the strain experienced in the ith cycle, i.e.

$$\Delta\varepsilon_i = 2\frac{\Delta_i}{L_c} \tag{9}$$

where Δ_i is defined as the value of cycle amplitude and L_c is the minimum core length. By replacing Eq. (9) into Eq. (8), and considering a negative value for parameter c (the fatigue ductility), we have

$$L_c \geq \left(\frac{1}{\varepsilon_f}\right) \times \lambda^{|c|} \tag{10}$$

where

$$\lambda = \left(2n_1 \times \Delta_1\left|\frac{1}{c}\right| + 2n_2 \times \Delta_2\left|\frac{1}{c}\right| + ... + 2n_m \times \Delta_m\left|\frac{1}{c}\right| \right) \quad (11)$$

For general metal, ε_f is defined as to the true strain of material fracture in tension (Mirtaheri *et al.* 2011). Eqs. (4) and (10) then provide the boundaries of optimal RL-BRB length.

2.3 Importance of the gap size

One of the important issues in designing RL-BRB is the determination of the size of the gap that has to be allowed between the central core and the concrete-encase. The concrete encases shall only act as lateral support to the core but not to take any role in carrying the load itself. The gap size affects the contact force of the buckled core acting on the concrete encase; an increase in the gap size might naturally happen due to elastic deformation of the encase during loading. Larger gap sizes result in higher contact forces and require higher stiffness and strength for the encase (Genna and Gelfi 2012, Jiang *et al.* 2015). In an effort, Jiang *et al.* (2015, 2017) conducted an analytical study regarding the influence of design parameters of BRBs and suggested the maximum gap size of 2 mm.

The gap can be filled with soft materials that allow the deformation of the core as it buckles under load. Researchers have suggested different materials for this such as epoxy resin, silicone resin, vinyl tapes, etc. though finally suggested silicon resin coating layer to fill the gap in the BRBs. Among other materials used by researchers in this regard, polystyrene foam, thin talc, coiling two-layer polyethylene film sheet with 0.15 by 0.2 mm thickness, butyl rubber sheet with 2 mm thickness, and so on can be named. In some cases, no material was used to fill the free space (Xie 2005).

3. Experimental study and Innovation

Reduced Length BRBs with nearly identical capacities in tension and compression have been designed as bracing segments (structural fuses), by having smaller capacities than that of buckling capacity of the bracing member, to improve the ductility and prevent initial buckling of the whole brace. While these fuses offer many advantages such as ductility and energy dissipation, they suffer from a key problem. The problem is that in these systems the whole brace capacity in both compression and tension is limited to the fuse capacity. The fuse capacity is designed according to the brace buckling capacity in compression which is even typically lower than its tensile capacity. Using RL-BRB reduce not only the axial compressive capacity of the bracing member but also its tensile capacity. Therefore, the overall lateral capacity of the braced frame shows substantial alteration when an RL-BRB is utilized. To gain higher values of tensile strength and enhance the fuse efficiency with regards to energy dissipation, innovative tensile elements were added to this fuse segment. Tension-only extra elements were used to eliminate the reduced tensile strength of the whole brace that exists in bracing elements which contain RL-BRB.

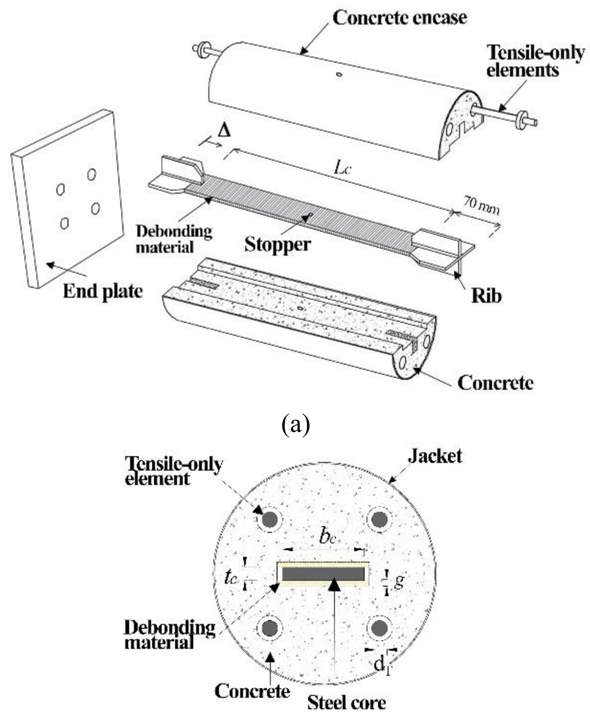

(a)

(b)

Fig. 6 CBRF components and cross-section

Based on the aforementioned information, a laboratory investigation was conducted to evaluate the performance of the single RL-BRB having tensile-only elements under cyclic loads as a Composite Buckling Restrained Fuse (CBRF). Fig. 6 shows the proposed CBRF components and cross-section. b_c, t_c are the width and thickness of the central core plate, d_T presents the tensile-only element's diameter and g is the gap size.

3.1 Innovative tensile elements

Provided that a concentric Chevron-braced frame, depicted in Fig. 7, is under a lateral load. Normally one of the bracing members will be under compression while the other one would be subjected to tension. In a condition that an RL-BRB is utilized in both of these diagonal braces as a hysteretic damper, the lateral load that is going to be gained by the braced frame would be limited to the sum of the horizontal component of the fuse capacities in compression and tension which is much lower than the bracing member capacity without fuse, either in tension or compression. With RL-BRB, the compressive and tensile capacities of the fuse are somehow similar and are limited to be lower than that of buckling capacity of the bracing member to ensure that the damage is confined in the fuse.

Additional tensile-only elements are utilized creatively in the proposed CBRF to make sure that the limitations in tension that exist in bracing members holding RL-BRBs are eliminated. The characteristic feature of the tensile-only elements is that they participate axially in bearing only in tension. The tensile capacity of the CBRF equipped with

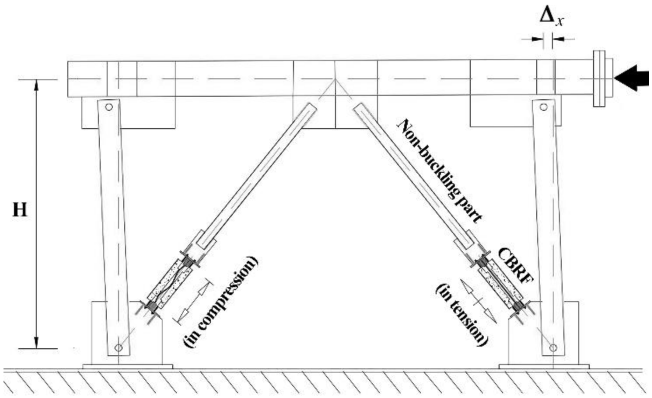

Fig. 7 Performance of CBRF in bracing members

tensile-only elements is designable. It could be designed according to the highest satisfactory tensile capacity of the bracing member corresponded to the anticipated story drift. Since the tensile capacity of the brace is normally greater than its compressive capacity, the expected tensile capacity of the proposed CBRF can be designed to be larger than its compressive capacity, Fig. 7. This increases the overall lateral capacity of the combination of tensile and compressive braces in comparison to when an RL-BRB is used.

3.2 Detailing and designing of the CBRF

3.2.1 Material

Base materials used in constructing of the CBRF was ST37-2 steel (DIN17100 1980) and ordinary concrete. Material properties of the steel core and steel tensile bar elements were derived from coupon testing of rectangular and circular samples loaded monotonically in tension (ASTM-E8 2016), shown in Fig. 8. A galvanized thin tube was considered for the jacket of the concrete encase as a mold. Since the space between the inner parts of the CBRF was small, workable concrete using plasticizer (0.5% liquid by weight of cement) with fine aggregates (less than 12 mm) was employed (Saberian *et al.* 2017, Haji *et al.* 2019, Kazemi *et al.* 2020a, Toghroli *et al.* 2020). Water to cement ratio of 0.50 and the slump of 70 mm was used to achieve the mix proportions. Evaporation protection was utilized for curing the concrete after placement (Jahandari *et al.* 2020). It should be noted that distilled water was utilized for characterization test and tap water for casting the samples since the water quality can have an important effect on the properties of the concrete (Jahandari *et al.* 2019a, Kazemi *et al.* 2020b, Rasekh *et al.* 2020). Concrete cube tests were conducted after 7 and 28 days of curing period (Jahandari *et al.* 2017, Jahandari *et al.* 2018, Jahandari *et al.* 2019b). A summary of the properties of the used materials is shown in Table 1.

3.2.2 Cross-sectional area and Concrete encase

Structural fuses are used to limit the structural failures to themselves while preserving the integrity of other components of the structure. The CBRF cross-sectional area, A_c, shall be designed by considering a strength modification

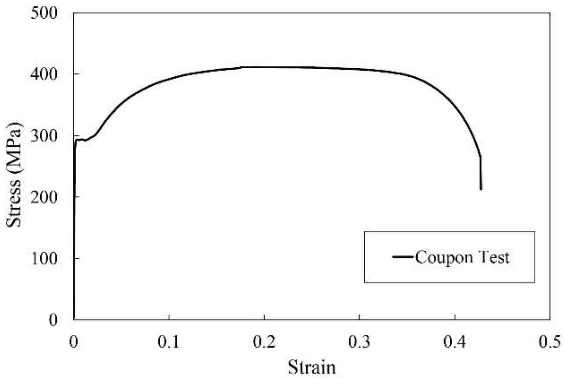

(a) Steel core plate

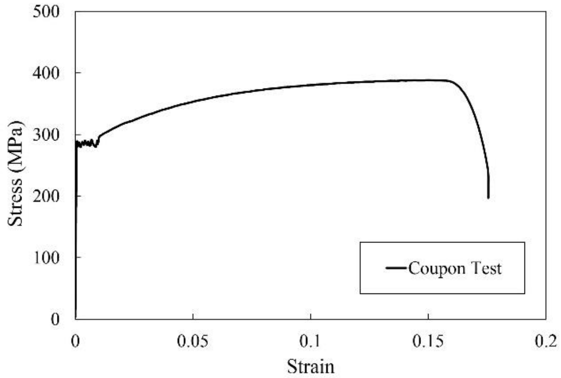

(b) Steel tensile bar

Fig. 8 Tensile response of coupon tests

factor, ψ, in a way that these sacrificial elements yield prior the whole brace buckling in compression or brace yielding under tension and dissipate the exposed energy. Since the compressive capacity of the bracing member is normally lower than its tensile capacity, the fuse needs to be designed according to the expected compressive capacity of the bracing member.

In order to make sure that yielding absolutely happens in the fuse, the strength diminution factor was taken as 0.7 (Kachooee and Kafi 2018). Assuming the frame depicted in Fig. 1(a), and employing the procedures of designing for CBFs in AISC341 (2016), Ozcelik *et al.* (2020) and also considering the limited states of global and local buckling for the bracing members in AISC360 (2016), the critical buckling load of the selected circular hollow section (CHS 60×3) with an approximate full-length of 1650 mm was calculated about 105kN in compression. Consequently, the CBRF cross-sectional area, A_c, was determined by Eq. (12).

$$A_c \leq \psi \frac{A_b \times F_{cre}}{F_y} \tag{12}$$

in which, A_b, is defined as the cross-section area of the brace (574 mm^2) and F_{cre}, is the brace buckling stress based on the expected yield stress of brace material calculated as 170MPa. F_y, presents the yield stress of CBRF core material. As per relevant calculations, the cross-sectional area of 210 mm^2 was obtained for the steel core and a thin steel plate (42×5 mm) was chosen for the samples.

Table 1 Material characterics of concrete and steel

Steel			Concrete	
	Core plate	Tensile-only bar		
Yield stress	290.38 MPa	285.10 MPa	Compressive strength at 7-days curing period	46.3 MPa
Ultimate Stress	411.63 MPa	388.37 MPa		
Module of Elasticity (0.2% offset (ASTM-E8 2016))	2.296×10^5 MPa	2.252×10^5 MPa	Compressive strength at 28-days curing period	51 MPa
Strain hardening	0.0174%	0.0105%		
Ultimate strain	25.02%	15.50%		

Based on the parametric investigations conducted by Jiang *et al.* (2015), 2 mm thick silicon resin was selected as the debonding material in order to fill the gap and avoid transition of shear force evidenced by Tsai and Weng (2002). CBRF core details are shown in Fig. 9.

Additional Tensile-only bars were used as a novelty in the proposed CBRF specimen so that to recover the undesirable limitation of bracing members in tensile force. Tensile-only bars need to be designed according to the satisfactory maximum tensile forces that would happen in the bracing member upon the predicted story drift. In this sample, four steel bars with a diameter of 8 mm (cumulative strength of 60kN), were utilized to achieve the satisfactory tensile strength of the anticipating 2% of frame story drift.

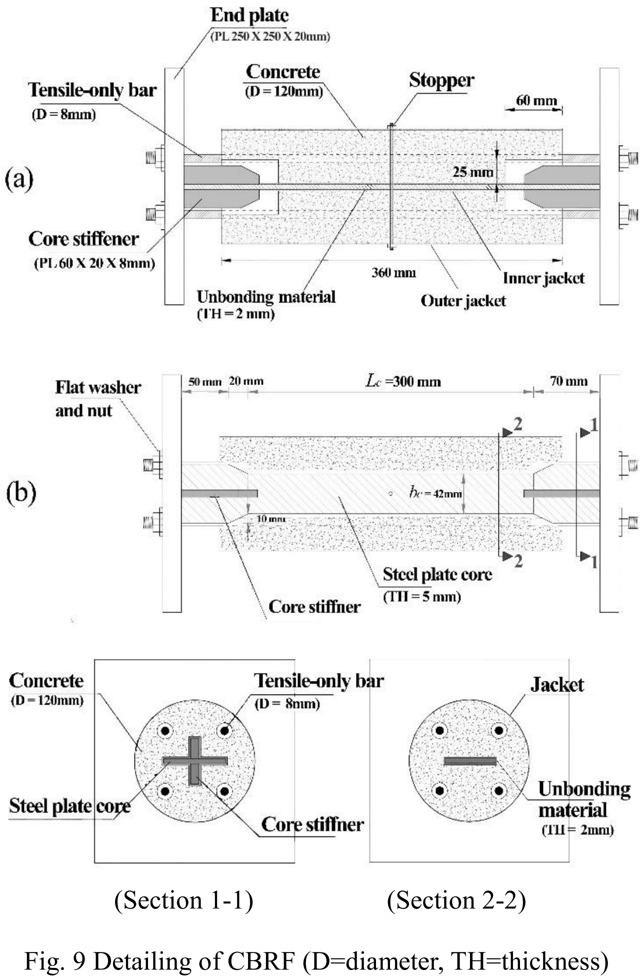

Fig. 9 Detailing of CBRF (D=diameter, TH=thickness)

The encasement shall be of sufficient strength and stiffness so that it does not deform relatively to the core. Encase must be designed for the contact forces that are exerted by the core as it buckles and makes contact with the encasement. Similar to the concepts that consider by the Robert Tremblay *et al.* (2006) and satisfying the criteria of Watanabe *et al.* (1988), a cylinder concrete encase by 120 mm diameter and 360 mm high was considered that shown in Fig. 9.

3.2.3 Length

CBRF core length is an important parameter that has a substantial impact on the energy absorption of the subjected load to the system (Tremblay *et al.* 2006, Mirtaheri *et al.* 2011). Owing to the short lengths of CBRF, for the same relative longitude core displacement, Δ, the average core strain, ε_{ca}, could be higher than that of longer full-length BRBs. The optimal core length can be measured according to its strain demand, ε_c, with regards to the maximum longitude displacement of the bracing member that holds CBRF corresponding to the frame story drift, θ, as shown in Eq. (13).

$$\Delta_b = (\theta \times \frac{\sin 2\phi}{2}) \times L_b \tag{13}$$

where Δ_b is defined as the longitude displacement of the full-length bracing member holding fuse, θ is the story drift, ϕ presents the bracing angle and L_b is the brace length.

Considering the story drift demand of 2% (AISC341 2016) under the Design Basis Earthquake (DBE) hazard level, Δ_b is assumed to be 16.20 mm for the bracing elements depicts in Fig. 1(a). Moreover, considering infinitive stiffness for the frame joints and taking A_{elastic}/A_c = 2.73, similar to concepts considered by Hoveidae *et al.* (2015) in Eq. (4) for the case with F_y = 290MPa, the core length ratio, $L_c/L_b \approx 0.2$ is obtained. To gain the predicted 5% of core demand (Mirtaheri *et al.* 2011, Razavi Tabatabaei *et al.* 2014) and satisfying the minimum brace deformation demand, L_c = 300 mm was considered for the samples.

It is important to point out that the chance of core fracture can be raised considerably due to the plastic behavior of the material because of low-cyclic fatigue (LCF) action (Takeuchi *et al.* 2008, Uriz 2008, Mirtaheri *et al.* 2011, Razavi Tabatabaei *et al.* 2014). In order to avoid the arising predicted fracture of the core, Eq. (10) needs to be considered.

Table 2 Parameters of sample

No.	Samples	Core Plate			Tensile-only bars	Restraining system
		L_c (mm)	b_c (mm)	t_c (mm)	d_T (mm)	g (mm)
1	RL-BRB	300	42	5	-	2
2	CBRF	300	42	5	8	2

3.3 Test samples

To investigate the performance of CBRF subjected to cyclic loading and earn insight into the use of additional tensile elements, a laboratory study was performed in which, two samples were designed, fabricated and tested. Fig. 9 depicts the properties of the samples mentioned in Table 2. The first sample as a control specimen was a Reduced Length Buckling Restrained Brace, RL-BRB, without tensile components while the second sample held tensile-only bars.

3.4 Loading history

The choice of a loading protocol depends on the purpose of the experiments, failure modes and type of the samples. In order to study the performance of the CBRF as a steel segment, ATC24 loading protocol was utilized (ATC24 1992). This standard loading protocol includes cycles which are a multiplier of the yield deformation, Δ_y, of the segment that was initially determined from the material properties mentioned. It follows by triple cycles with amplitudes of 0.5, 0.75, 1, 2, 3, 4 yield deformation, Δ_y, of the core and double cycles with amplitudes of 6, 8, 11, 14, 18, 22, 27, 32, 38, 44 Δ_y which shown in Fig. 10. According to the loading protocol mentioned, Eq. (8) can be re-written as follow:

$$\frac{3}{\frac{1}{2}\times(\frac{\Delta_y}{L_c\varepsilon_f})^{\frac{1}{c}}}+\frac{3}{\frac{1}{2}\times(\frac{2\Delta_y}{L_c\varepsilon_f})^{\frac{1}{c}}}+\dots + \frac{2}{\frac{1}{2}\times(\frac{6\Delta_y}{L_c\varepsilon_f})^{\frac{1}{c}}}+\frac{2}{\frac{1}{2}\times(\frac{8\Delta_y}{L_c\varepsilon_f})^{\frac{1}{c}}}+\dots\leq 1 \tag{14}$$

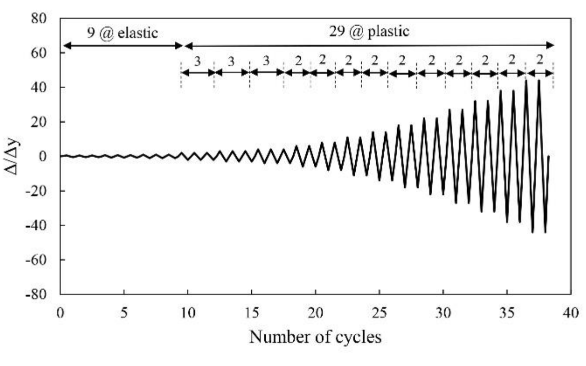

Fig. 10 Load-deformation protocol (ATC24 (1992))

Since c has a negative value, Eq. (14) can be modified to:

$$\begin{pmatrix} 6\times(1)^{\left|\frac{1}{c}\right|}+6\times(2)^{\left|\frac{1}{c}\right|}+\dots \\ +4\times(6)^{\left|\frac{1}{c}\right|}+4\times(8)^{\left|\frac{1}{c}\right|}+\dots \end{pmatrix}\times\left[(\frac{\Delta_y}{L_c\varepsilon_f})^{\left|\frac{1}{c}\right|}\right]\leq 1 \tag{15}$$

The yielding core deformation was set to Δ_y = 0.38 mm and ε_f= 0.25 according to the material properties mentioned for the steel core, Table 1, and coefficient c was taken as -0.458 reported by the Uriz (2008). In order to prevent the core fracture due to low-cyclic fatigue, the core, the core length was calculated as $L_c \geq$ 212 mm which acknowledged the considered core length of 300 mm.

3.5 Test setup

The uniaxial test setup consists of a hydraulic jack capable of exerting cyclically up to a maximum of 1000 kN tensile load and a maximum of 2000 kN compressive load while accommodating a maximum stroke of ±100 mm. It was also equipped with a 1000 kN load-cell. As depicted in Fig. 11, this setup consists of two reaction steel blocks which were connected to the strong floor with bolts and two lines of rails that wagons ride on it. Linear guide-way (wagon) was used to avoid the lateral displacement of the load cell and jack and apply the load axially to the sample without any rotation.

In order to create area for placing the tensile elements behind the endplate, four steel bushes with a height of 50 mm were placed on each side of the CBRF sample though they were not considered for the RL-BRB test since the RL-BRB did not contain the additional tensile elements.

Two high accuracy LVDTs were installed on the endplate to monitor the exact longitude displacement. Moreover, two other LVDTs were mounted to investigate the horizontal and vertical deformation of the concrete encasement. It should be noted that all of the equipment was calibrated before the test. Fig. 11(b) shows the assembled CBRF sample in the setup.

4. Experiment results and discussions

The hysteretic curve of the samples are presented in Figs. 12(a) and 12(b), where the failure points of the samples are shown with a red triangle. Figs. 12(c) and 12(d) presents the comparison of the energy-loading and backbone curves of the hysteretic response of the RL-BRB and CBRF. The hysteresis results of two samples were explored closely. The RL-BRB, sample 1, was the control specimen without tensile-only bars to compare the performance of another sample. As presented in Fig. 12(a), the hysteretic loops of sample 1 are stable and steady without pinching. This behavior was similar to RL-BRB tested by Mirtaheri *et al.* (2011). The fuse has the same capacity in the compression and tension with favorable ductility. The axial bearing ratio is defined as P/P_y, in which P_y is the product of core area, A_c and core yield stress, F_y and P is the axial force. The maximum axial bearing ratios,

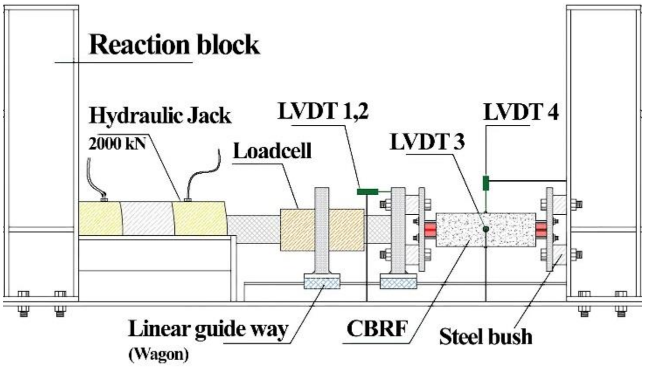

(a) Schematic of the test setup

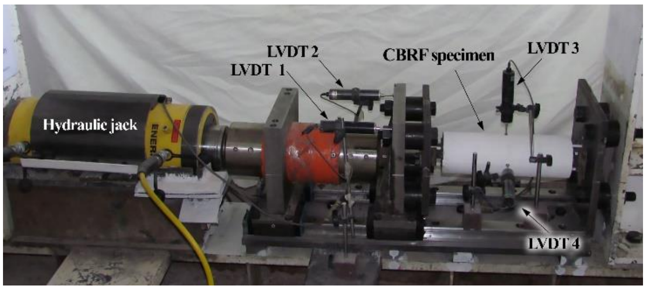

(b) Assembled CBRF sample in setup

Fig. 11 Proposed CBRF test setup

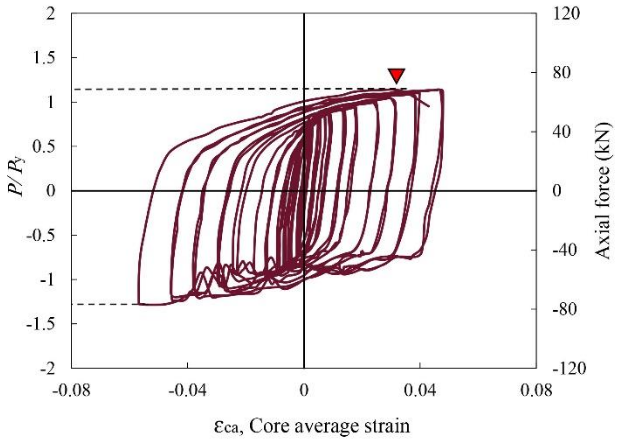

(a) Hysteretic response of RL-BRB

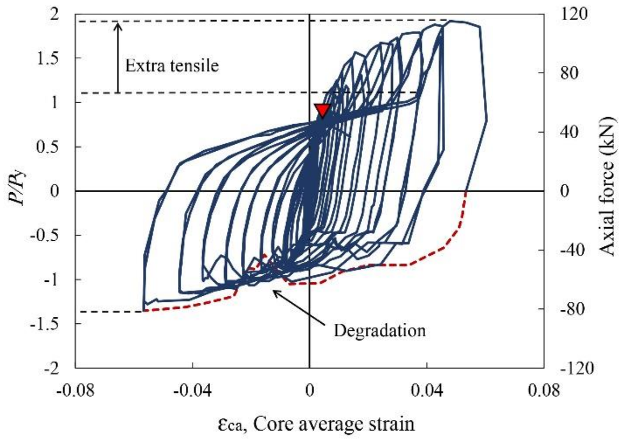

(b) Hysteretic response of CBRF

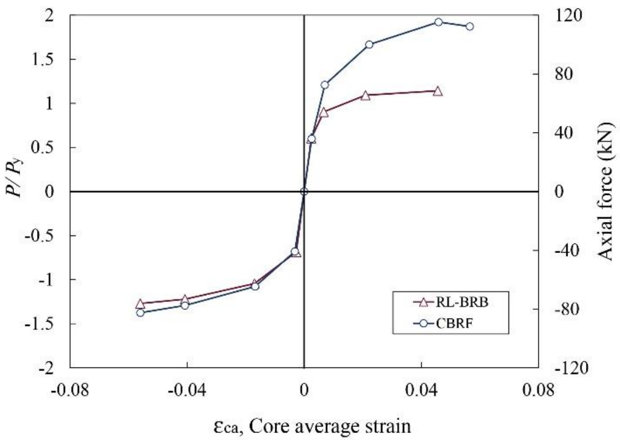

(c) Comparison of backbone curves

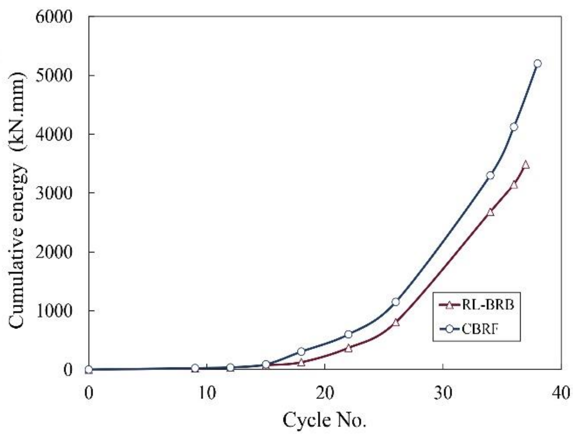

(d) Comparison of energy-loading curves

Fig. 12 The Hysteretic response and comparison energy-loading of and backbone curves of the samples

P/P_y, of RL-BRB are 1.12 in tension and 1.27 in compression. Sawtooth parts of the curve demonstrate the resulting degradation during the buckling of the core in the compressive phase. The maximum inelastic average core strain at the end of 36 cycles is 0.048, which is interpreted by the appropriate behavior of the core in energy dissipation and ductility. Besides using the features of the buckling-restrained mechanism in the compression phase, using extra tensile elements in CBRF are caused that the tensile capacity of the fuse increases to its desired amount. As presented in Fig. 12(b), the hysteretic loops similar to sample 1 which has a desired enhancement on the energy dissipation and a favorable tensile strength.

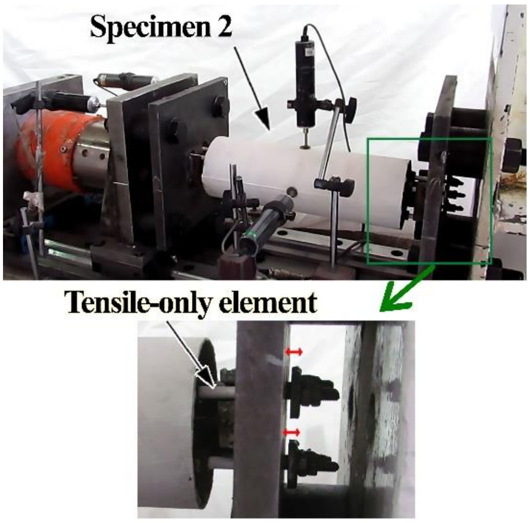

(a) Performance of tensile elements in compression

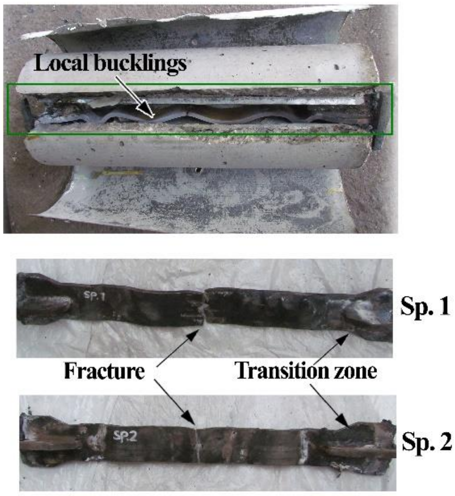

(b) Deformed shape of the cores after test

Fig.13 Test observations

The maximum axial compressive bearing ratio of the CBRF is 1.35 which occurs at the core strain of 0.055. This has been achieved by the core alone as the extra tensile elements are not involved in carrying the load in compression, Fig. 13(a). The maximum tensile axial force of the CBRF, sample 2, was obtained as 115 kN which is close to the desired tensile amount of the bracing member. Prior to the deformation passing the elastic zone at the 9th cycle, the bearing ratios in compression and tension are almost similar while beyond Δ_y, at the 10th cycles, the compressive and tensile bearing ratios, P/P_y, become different and their difference growing rapidly.

In the 33rd cycle with 32Δy it is about 60 kN due to additional tensile bars. The maximum average core strain exhibited by the CBRF and RL-BRB were 0.048 and 0.055, respectively.

The CBRF satisfied the primarily aim of this study to achieve higher tensile strength without major changes in the compressive capacity of the fuse, Fig. 12(c). This hysteretic damper with high potential of energy dissipation possess various capacities in compression and tension. In comparison to the RL-BRB, using additional tensile-only elements could stretch the tensile zone of the hysteretic curves and enhances the energy dissipation of the system. Fig. 12(d) shows the cumulative hysteretic energy dissipation of the specimens for a maximum of the 38th cycle corresponding to 0.055 core average strain. As expected, the CBRF with extra tensile elements exhibited higher energy dissipation. The CBRF dissipated cumulative energy of 4125 kN.mm, whereas the RL-BRB sample showed 3151 kN.mm at the end of 36th cycle. It’s quite logical that the efficiency expected in the proposed CBRF is not significantly higher than RL-BRB and resulting from the design conditions of extra tensile-only bars. Depending on the desired tensile strength of the brace element with respect to the expected story drift, the CBRF could achieve higher tensile strength.

The fuse satisfied the allowable story drift limit of 2% for the frame as mentioned previously. The core plate was investigated closely when the sample was dismantled, Fig. 13(b). The steel plate core experienced symmetrical sinusoidal waves, and there was no buckling in the transition zone.

4.1 load carrying capacity

The maximum load-carrying capacity of the sample in consecutive cycles indicates the fuse ability to resist axial loading (Mirtaheri *et al.* 2011, Rahai and Mortazavi 2014). Fig. 14(a) depicts the maximum capacity of the fuse in tension and compression during cycles. As expected, the CBRF containing tensile-only elements exhibited greater tensile strength during the plastic cycles. This performance could compensate for the reduced tensile strength of the bracing element with respect to its desired tensile capacity.

4.2 Strength adjustment factors

Strength adjustment factors indicate the magnitude of maximum forces associated with BRBs for design purposes. (Pandikkadavath and Sahoo 2016a, b). Two types of strength adjustment factors are defined by AISC341 (2016). Tension strength adjustment factor (ω) denotes the strain hardening of the BRB which is defined as the ratio of maximum tensile force (T_{max}) to the core yield force, P_y, at the same strain level, Eq. (16).

$$\omega = \frac{T_{\max}}{P_y} \tag{16}$$

Fig. 14(b) illustrates the variation of ω corresponding to the average core strain of the samples. The values of ω for the RL-BRB and CBRF were calculated to be 1.1 and 1.92 at core strains of 0.048 and 0.055 respectively. This difference comes the utilization of tensile-only element in the proposed CBRF. The compression strength factor (β) can be calculated as the ratio of maximum compressive force (C_{max}) to the corresponding maximum tensile force (T_{max}) at the same strain level, Eq. (17).

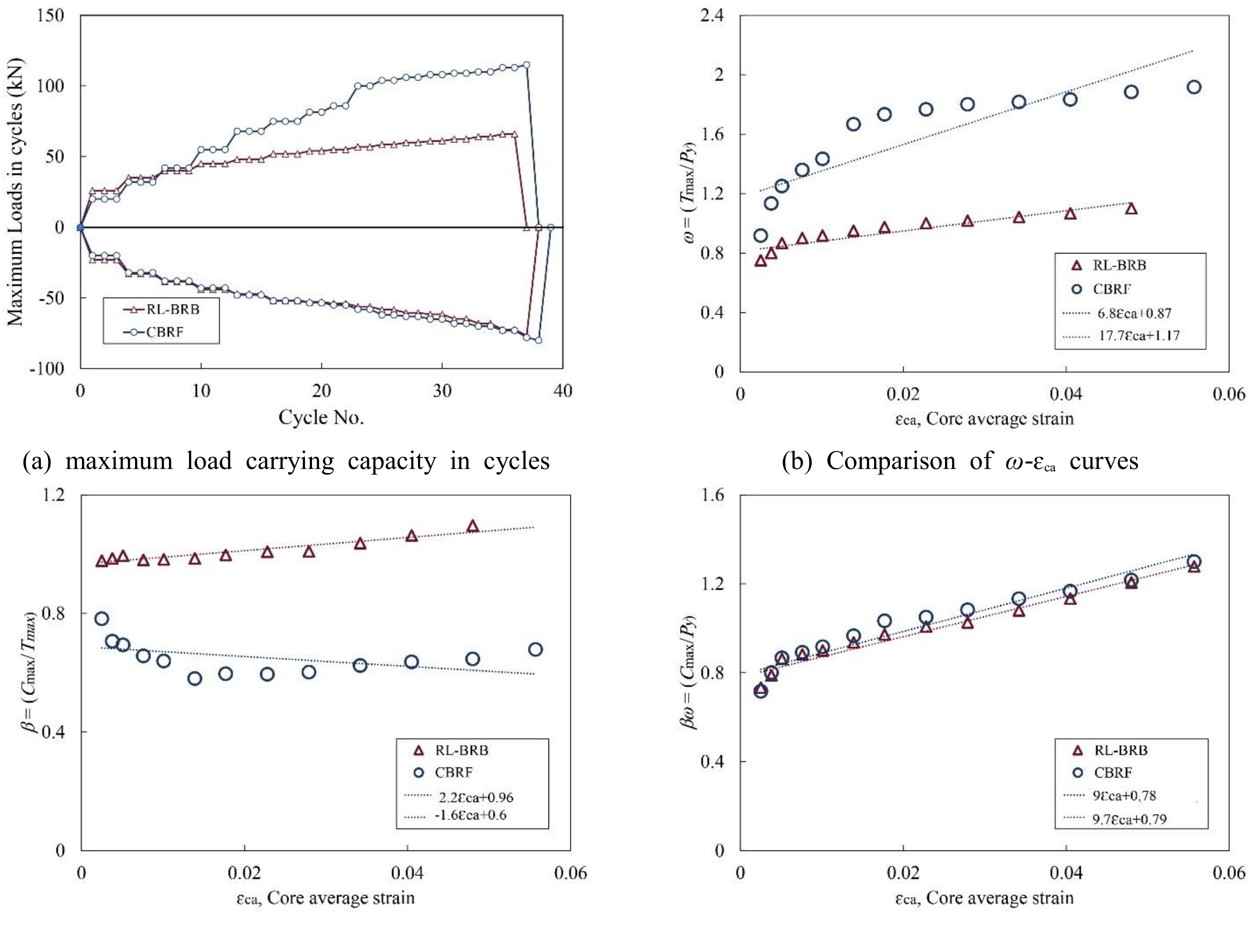

(a) maximum load carrying capacity in cycles

(b) Comparison of ω-ε_{ca} curves

(c) Comparison of β-ε_{ca} curves

(d) Comparison of $\beta\omega$-ε_{ca} curves

Fig. 14 Load carrying capacity and comparison of adjustment factors plots with ε_{ca} of the sampless

$$\beta = \frac{C_{\max}}{T_{\max}} \tag{17}$$

Fig. 14(c) shows the variation of β with the average core strain of the samples. The average maximum values of the β for the RL-BRB and CBRF were found to be 1.1 and 0.68 at the core strains of 0.048 and 0.055 respectively.

As shown in Fig. 14(c), the compression strength factor of the CBRF was decreased till the average core strain of 0.0139, beyond which a gradual increase was noticed with the increasing level of the average core strain. Total strength adjustment factor in compression is defined as the product of β and ω. This factor represents the combined effect of Poisson and strain hardening effect which governs the maximum design capacity of the BRBs (Pandikkadavath and Sahoo 2016b). Fig. 14(d) depicts the relationship between the $\beta\omega$ and ε_{ca}. The test data were fitted with the trend lines having a generalized form related to the average core strain (εca).

4.3 Damping potential

As noted earlier, CBRF can be used as a damper having a hysteretic behavior to absorb the energy. Damping potential of the samples can be quantified from their corresponding hysteretic response to be used in structural design procedures.

The enclosed area under the hysteretic cycles indicates the energy dissipated by the samples. The equivalent viscous damping index, β_{eff}, of the samples can be calculated from the energy dissipated in each plastic cycle using FEMA356 (2000) provision as given below

$$\beta_{eff} = \frac{1}{2\pi}\frac{W_D}{K_{eff}\Delta^2_{ave}} \tag{18}$$

where W_D is defined as an area surrounded by a whole cycle of the load-deformation response of sample and Δ_{ave} is the average of the absolute amounts of the displacement that the sample gained due to this cycle. Equivalent axial stiffness, K_{eff}, is defined as the following

$$K_{eff} = \frac{|F^-| + |F^+|}{|\Delta^-| + |\Delta^+|} \tag{19}$$

where F^- and F^+ are defined as the maximum compressive and tensile forces, while the Δ^- and Δ^+ are defined as the corresponded maximum displacement due to compressive and tensile displacements in every cycle, orderly. Fig. 15

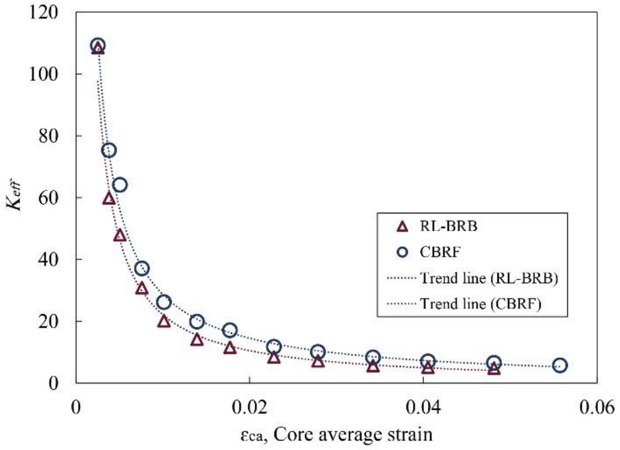

(a) equivalent axial stiffness

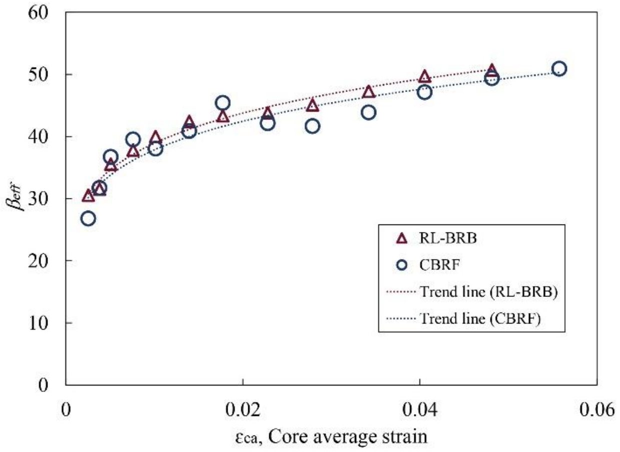

(b) equivalent viscous damping

Fig. 15 Damping potential of the samples in each cycle

shows the variations of the K_{eff} and β_{eff} of the samples with the average core strain. The CBRF exhibited higher K_{eff} at every loading cycle in comparison to the RL-BRB. The equivalent axial stiffness of the samples showed a gradual decrease with the raising magnitude of average core strain. The maximum amounts of K_{eff} showed by the BL-BRB and CBRF were around 110 kN/mm. The equivalent viscous damping, β_{eff}, of the samples exhibited a gradual increment with the raising amounts of the average core stain. The maximum amount of the β_{eff} was 50.90% for the CBRF sample at the corresponding average core strain of 0.055.

5. Conclusions

Fuse or sacrificial elements are the weakest part of a structure that are designed to fail at certain loads and in certain modes. These elements can be designed to locally absorb and dissipate the energy of an extreme load applied to the system thereby reducing or eliminating damage to the rest of the structure. Composite Buckling-restrained fuse (CBRF), proposed here, is an axial innovative structural fuse which is an enhancement on the reduced-length buckling-restrained braces (RL-BRBs). The main difference is that it exhibited different capacities in tension and compression. Utilizing extra tensile-only elements in an innovative configuration enhances the energy dissipation efficiency and alleviates the tensile strength reduction of the bracing members containing RL-BRBs as a structural fuse. Design provisions and detailing of the proposed CBRF was elaborated. The study continued with an experimental program for the proposed CBRF compared with RL-BRB. Some key design parameters regarding these were discussed as well. The results of the study are listed.

- This research proposed theoretical equations for determining the optimal boundaries of BRB length considering the elastoplastic behavior of the steel core and low-cyclic fatigue phenomena.
- Tension-only extra elements are utilized innovatively in the suggested CBRF to ensure that no reduction would occur in the satisfactory tensile load of the bracing elements unlike what occurs when an RL-BRB fuse is used. The characteristic feature of the tension-only elements is that they participate in bearing only in tension.
- Single CBRF and RL-BRB samples were tested experimentally. The findings show that CBRF offers favorable improvement in the energy dissipation and tensile capacity along with reasonably stable hysteretic response subjected to cyclic loads. The maximum average core strain exhibited by the RL-BRB and CBRF were 0.048 and 0.055, respectively. Proposed CBRF gained maximum amount of 50.90% for the equivalent viscous damping parameter corresponded to the average core stain of 0.055.
- The maximum values of the tensile-strength adjustment factor, ω, were 1.11 and 1.92 for the RL-BRB and CBRF, respectively. The compression adjustment factor, β, reached by the respective samples were 1.1 and 0.68. These differences come from the utilization of tensile-only elements in the proposed CBRF.

Low cost of the rebuild, workability, and ease of use are the most fundamental features of a fuse, all of which are present in the composite buckling-restrained fuse (CBRF) with extra tensile-only elements that is proposed in this research. However, more research is recommended to be conducted on some key parameters such as the core-length. The suggested structural fuse is made of conventional materials and can be cast using a simple manufacturing process. Both of these can be claimed as advantages of this axial hysteretic damper.

References

Abdel Raheem, S. and Hayashikawa, T. (2013) “Energy dissipation system for earthquake protection of cable-stayed bridge towers”, *Earthq. Struct.*, **5**(6), 657-678. https://doi.org/10.12989/eas.2013.5.6.657.

AISC341 (2016), *ANSI/AISC 341-16, Seismic Provisions for Structural Steel Buildings,* United States of America, Chicago: American Institute of Steel Construction.

AISC360 (2016), *ANSI/AISC 360-16, Specification for Structural Steel Buildings*, United States of America, Chicago: American Institute of Steel Construction.

Andalib, Z., Kafi, M.A., Kheyroddin, A. and Bazzaz, M. (2014), "Experimental investigation of the ductility and performance of steel rings constructed from plates", *J. Constr. Steel Res.*, **103**, 77-88. https://doi.org/10.1016/j.jcsr.2014.07.016.

Andalib, Z., Kafi, M.A., Kheyroddin, A., Bazzaz, M. and Momenzadeh, S. (2018), "Numerical evaluation of ductility and energy absorption of steel rings constructed from plates", *Eng. Struct.*, **169**, 94-106. https://doi.org/10.1016/j.engstruct.2018.05.034.

ASTM-E8 (2016), *ASTM E8/E8M-16a, Standard Test Methods for Tension Testing of Metallic Materials*, West Conshohocken, PA.

ATC24 (1992) *Guidelines for cyclic seismic testing of components of steel structures*, Redwood City, Calif.: Applied Technology Council.

Bahirai, M. and Gerami, M. (2019), "An experimental and numerical investigation on seismic retrofit of steel moment frame connections", *J. Earthq. Eng.*, 1-21. https://doi.org/10.1080/13632469.2019.1616336.

Bazzaz, M., Andalib, Z., Kafi, M.A. and Kheyroddin, A. (2015a), "Evaluating the performance of OBS-C-O in steel frames under monotonic load", *Earthq. Struct.*, **8**(3), 697-710. http://dx.doi.org/10.12989/eas.2015.8.3.697

.Bazzaz, M., Andalib, Z., Kafi, M.A. and Kheyroddin, A. (2015b), "Numerical comparison of the seismic performance of steel rings in off-centre bracing system and diagonal bracing system", *Steel Compos. Struct.*, **19**(4), 917-937. http://dx.doi.org/10.12989/scs.2015.19.4.917.

Bazzaz, M., Kheyroddin, A., Kafi, M.A. and Andalib, Z. (2012), "Evaluation of the seismic performance of off-centre bracing system with ductile element in steel frames", *Steel Compos. Struct.*, **12**(5), 445-464. http://dx.doi.org/10.12989/scs.2012.12.5.445.

Bergami, A. and Nuti, C. (2013), "A design procedure of dissipative braces for seismic upgrading structures", *Earthq. Struct.*, **4**, 85-105.

Bonetti, S. (2008), *Ductile fuses for special concentrically braced frames*, unpublished thesis (Doctor of Philosophy), University of Kansas.

Bruneau, M., Uang, C.M. and Sabelli, R. (2011), *Ductile Design of Steel Structures*, 2nd Ed., McGraw-Hill Education.

Budynas, R.G., Nisbett, J.K. and Shigley, J.E. (2011), *Shigley's mechanical engineering design*, 9th Ed., New York: McGraw-Hill.

Calado, L., Proença, J., Espinha, M. and Castiglioni, C. (2013) "Hysteretic behavior of dissipative welded fuses for earthquake resistant composite steel and concrete frames", *Steel Compos. Struct.*, **14**(6), 547-569. http://dx.doi.org/10.12989/scs.2013.14.6.547.

.Craighead, G. (2009), 'Chapter 1 - High-Rise Building Definition, Development, and Use' in *High-Rise Security and Fire Life Safety (Third Edition)*, Boston: Butterworth-Heinemann, 1-26.

Deihim, M. and Kafi, M.A. (2017), "A parametric study into the new design of a steel energy-absorbing connection", *Eng. Struct.*, **145**, 22-33. https://doi.org/10.1016/j.engstruct.2017.04.056.

DIN17100 (1980), *DIN 17100, Steels for general structural purposes-Quality Standard*.

Dizaj, E., Fanaie, N. and Zarifpour, A. (2017), "Probabilistic seismic demand assessment of steel frames braced with reduced yielding segment buckling restrained braces", *Adv. Struct. Eng.*, **21**(7), 1002-1020. https://doi.org/10.1177/1369433217737115.

Dougka, Y., Dimakogianni, D. and Vayas, I. (2014), "Seismic behavior of frames with innovative energy dissipation systems (FUSEIS 1-1)", *Earthq. Struct.*, **6**(5), 561-580. https://doi.org/10.12989/eas.2014.6.5.561.

EERI. (1995), "Northridge Earthquake Reconnaissance Report. Vol. 1.", *Earthq. Spectra*, supplement C to vol. 11.

Engelhardt, M.D. and Sabol, T.A. (1995), *Testing of welded steel moment connections in response to the northridge earthquake*: Progress Report to the AISC Advisory Committee on Special Moment-Resisting Frame Research.

Engelhardt, M.D. and Sabol, T.A. (1998), "Reinforcing of steel moment connections with cover plates: benefits and limitations", *Eng. Struct.*, **20**(4-6), 510-520. https://doi.org/10.1016/S0141-0296(97)00038-2.

Fanaie, N. and Dizaj, E. (2014), "Response modification factor of the frames braced with reduced yielding segment BRB", *Struct. Eng. Mech.*, **50**(1), 1-17. http://dx.doi.org/10.12989/sem.2014.50.1.001

.FEMA356 (2000), *Prestandard and Commentary for the Seismic Rehabilitation of Buildings*, Washington, DC.: Federal Emergency Management Agency.

Fujimoto, M., Wada, A., Saeki, E., Watanabe, A. and Hitomi, Y. (1988), "A study on the unbonded brace encased in buckling restraining concrete and steel tube", *J. Struct. Constr. Eng.*, 249-258.

Genna, F. and Gelfi, P. (2012), "Analysis of the lateral thrust in bolted steel buckling-restrained braces. I: Experimental and numerical results", *J. Struct. Eng.*, **138**(10), 1231-1243. https://doi.org/10.1061/(ASCE)ST.1943-541X.0000558.

Gorji Azandariani, M., Abdolmaleki, H. and Gorji Azandariani, A. (2020a), "Numerical and analytical investigation of cyclic behavior of steel ring dampers (SRDs)", *Thin-Wall. Struct.*, **151**, 106751. https://doi.org/10.1016/j.tws.2020.106751.

Gorji Azandariani, M., Gorji Azandariani, A. and Abdolmaleki, H. (2020b), "Cyclic behavior of an energy dissipation system with steel dual-ring dampers (SDRDs)", *J. Constr. Steel Res.*, **172**, 106145. https://doi.org/10.1016/j.jcsr.2020.106145.

Grigorian, C.E., Yang, T.S. and Popov, E.P. (1993), "Slotted Bolted Connection Energy Dissipators", *Earthq. Spectra*, **9**(3), 491-504.

Haji, M., Naderpour, H. and Kheyroddin, A. (2019), "Experimental study on influence of proposed FRP-strengthening techniques on RC circular short columns considering different types of damage index", *Compos.Struct.*, **209**, 112-128. https://doi.org/10.1016/j.compstruct.2018.10.088.

Hashin, Z. and Rotem, A. (1978), "A cumulative damage theory of fatigue failure", *Mater. Sci. Eng.*, **34**(2), 147-160.

Hoveidae, N. (2018), "Numerical investigation of seismic response of hybrid buckling restrained braced frames", *Periodica Polytechnica Civil Engineering*, **63**(1). https://doi.org/10.3311/PPci.12040.

Hoveidae, N., Tremblay, R., Rafezy, B. and Davaran, A. (2015), "Numerical investigation of seismic behavior of short-core all-steel buckling restrained braces", *J. Constr. Steel Res.*, **114**, 89-99. https://doi.org/10.1016/j.jcsr.2015.06.005.

Jahandari, S., Li, J., Saberian, M. and Shahsavarigoughari, M. (2017), "Experimental study of the effects of geogrids on elasticity modulus, brittleness, strength, and stress-strain behavior of lime stabilized kaolinitic clay", *Geo Res J*, **13**, 49-58. https://doi.org/10.1016/j.grj.2017.02.001.

Jahandari, S., Mojtahedi, S.F., Zivari, F., Jafari, M., Mahmoudi, M.R., Shokrgozar, A., Kharazmi, S., Vosough Hosseini, B., Rezvani, S. and Jalalifar, H. (2020), "The impact of long-term curing period on the mechanical features of lime-geogrid treated soils", *Geomech. Geoeng.*, 1-13. https://doi.org/10.1080/17486025.2020.1739753.

Jahandari, S., Saberian, M., Tao, Z., Mojtahedi, S.F., Li, J., Ghasemi, M., Rezvani, S.S. and Li, W. (2019a), "Effects of saturation degrees, freezing-thawing, and curing on geotechnical properties of lime and lime-cement concretes", *Cold Regions Sci. Technol.*, **160**, 242-251. https://doi.org/10.1016/j.coldregions.2019.02.011.

Jahandari, S., Saberian, M., Zivari, F., Li, J., Ghasemi, M. and Vali, R. (2019b), "Experimental study of the effects of curing time on geotechnical properties of stabilized clay with lime and geogrid", *Int. J. Geotech. Eng.*, **13**(2), 172-183. https://doi.org/10.1080/19386362.2017.1329259.

Jahandari, S., Toufigh, M.M., Li, J. and Saberian, M. (2018), "Laboratory study of the effect of degrees of saturation on lime concrete resistance due to the groundwater level increment", *Geotech. Geological Eng.*, **36**(1), 413-424. https://doi.org/10.1007/s10706-017-0335-4.

Jiang, Z., Guo, Y., Zhang, B. and Zhang, X. (2015), "Influence of design parameters of buckling-restrained brace on its performance", *J. Constr. Steel Res.*, **105**, 139-150. https://doi.org/10.1016/j.jcsr.2014.10.024.

Jiang, Z.Q., Dou, C., Guo, Y.L. and Zhang, A.L. (2017), "Theoretical study on design methods for pinned assembled BRB with flat core", *Eng. Struct.*, **133**, 1-13. https://doi.org/10.1016/j.engstruct.2016.12.004.

Jurukovski, D., Petkovski, M. and Rakicevic, Z. (1995), "Energy absorbing in regular and composite steel frame structures", *Eng. Struct.*, **17**, 319-333.

Kachooee, A. and Kafi, M.A. (2018), "A suggested method for improving post buckling behavior of concentric braces based on experimental and numerical studies", *Structures*, **14**, 333-347. https://doi.org/10.1016/j.istruc.2018.04.003.

Karalis, A. and Stylianidis, K. (2013), "Experimental investigation of existing R/C frames strengthened by high dissipation steel link elements", *Earthq. Struct.*, **5(2)**, 143-160. https://doi.org/10.12989/eas.2013.5.2.143.

Kazemi, M., Hajforoush, M., Talebi, P.K., Daneshfar, M., Shokrgozar, A., Jahandari, S., Saberian, M. and Li, J. (2020a), "In-situ strength estimation of polypropylene fibre reinforced recycled aggregate concrete using Schmidt rebound hammer and point load test", *J. Sustainable Cement-Based Materials*, 1-18. https://doi.org/10.1080/21650373.2020.1734983.

Kazemi, M., Li, J., Lahouti Harehdasht, S., Yousefieh, N., Jahandari, S. and Saberian, M. (2020b), "Non-linear behaviour of concrete beams reinforced with GFRP and CFRP bars grouted in sleeves", *Structures*, **23**, 87-102. https://doi.org/10.1016/j.istruc.2019.10.013.

Kim, J., Choi, H. and Chung, L. (2004), "Energy-based seismic design of structures with buckling-restrained braces", *Steel Compos. Struct.*, **4**(6), 437-452. https://doi.org/10.12989/scs.2004.4.6.437.

Maalek, S., Heidary-Torkamani, H., Pirooz, M. and Naeeni, S.T.O. (2019), "Numerical investigation of cyclic performance of frames equipped with tube-in-tube buckling restrained braces", *Steel Compos. Struct.*, **30**(3), 201-215. https://doi.org/10.12989/scs.2019.30.3.201.

Mete Güneyisi, E., Tunca, O. and Azez, I. (2015), "Nonlinear dynamic response of reinforced concrete building retrofitted with buckling restrained braces", *Earthq. Struct.*, **8**(6), 1349-1362. https://doi.org/10.12989/eas.2015.8.6.1349.

Mirtaheri, M., Gheidi, A., Zandi, A.P., Alanjari, P. and Samani, H.R. (2011), "Experimental optimization studies on steel core lengths in buckling restrained braces", *J. Constr. Steel Res.*, **67**(8), 1244-1253. https://doi.org/10.1016/j.jcsr.2011.03.004.

Mohammadi, M., Kafi, M.A. and Kheyroddin, A. (2017), *Innovative composite buckling-restrained structural fuse (CBRF) with different capacity in tension and compression*, Patent Number: 91536, Iranian organization for registration of deeds and properties.

Mohammadi, M., Kafi, M.A., Kheyroddin, A. and Ronagh, H.R. (2018a), 'Experimental Study of Innovative Composite Buckling-Restrained Fuse for Concentrically Braced Frames Under Cyclic Load', in *ASEA-SEC 04*, Queensland, Australia, ISEC Press.

Mohammadi, M., Kafi, M.A., Kheyroddin, A. and Ronagh, H.R. (2019), "Experimental and numerical investigation of an innovative buckling-restrained fuse under cyclic loading", *Structures*, **22**, 186-199. https://doi.org/10.1016/j.istruc.2019.07.014.

Mohammadi, M., Kafi, M.A., Kheyroddin, A., Ronagh, H.R. and Rashidi, M. (2018b), "Experimental and numerical investigation of innovative composite buckling-restrained fuse", in *ACMSM25*, Brisbane, Australia, springer.

Mualla, I.H. and Belev, B. (2002), "Performance of steel frames with a new friction damper device under earthquake excitation", *Eng. Struct.*, **24**(3), 365-371. https://doi.org/10.1016/S0141-0296(01)00102-X.

Ozcelik, R., Dikiciasik, Y., Civelek, K.B., Erdil, E.F. and Erdal, F. (2020) "Design of buckling restrained braces with composite technique", *Steel Compos. Struct.*, **35**(5), 687-699. https://doi.org/10.12989/scs.2020.35.5.687.

Pall, A.S. and Marsh, C. (1982), "Response of Friction Damped Braced Frames", *J. Struct. Division*, **108**(6), 1313-1323.

Pandikkadavath, M.S. and Sahoo, D.R. (2016a), "Analytical investigation on cyclic response of buckling-restrained braces with short yielding core segments", *Int. J. Steel Struct.*, **16**, 1273-1285. https://doi.org/10.1007/s13296-016-0083-y.

Pandikkadavath, M.S. and Sahoo, D.R. (2016b), "Cyclic testing of short-length buckling-restrained braces with detachable casings", *Earthq. Struct.*, **10**(3), 699-716. http://dx.doi.org/10.12989/eas.2016.10.3.699.

Pandikkadavath, M.S. and Sahoo, D.R. (2017), "Mitigation of seismic drift response of braced frames using short yielding-core BRBs", *Steel Compos. Struct.*, **23**(3), 285-302. https://doi.org/10.12989/scs.2017.23.3.285.

Park, J., Lee, J. and Kim, J. (2012), "Cyclic test of buckling restrained braces composed of square steel rods and steel tube", *Steel Compos. Struct.*, **13**(5), 423-436. https://doi.org/10.12989/scs.2012.13.5.423.

Rahai, A.R. and Mortazavi, M. (2014), "Experimental and numerical study on the effect of core shape and concrete cover length on the behavior of BRBs", *Int. J. Civil Eng.*, **12**(4), 379-395.

Rasekh, H., Joshaghani, A., Jahandari, S., Aslani, F. and Ghodrat, M. (2020), '2 - Rheology and workability of SCC' in Siddique, R., ed., *Self-Compacting Concrete: Materials, Properties and Applications* Woodhead Publishing, 31-63.

Rashidi, M., Ghodrat, M., Samali, B. and Mohammadi, M. (2018), 'Decision Support Systems' in *Management of information systems* IntechOpen.

Razavi Tabatabaei, S.A., Mirghaderi, S.R. and Hosseini, A. (2014), "Experimental and numerical developing of reduced length buckling-restrained braces", *Eng. Struct.*, **77**, 143-160. https://doi.org/10.1016/j.engstruct.2014.07.034.

Saberian, M., Jahandari, S., Li, J. and Zivari, F. (2017), "Effect of curing, capillary action, and groundwater level increment on geotechnical properties of lime concrete: Experimental and prediction studies", *J. Rock Mech. Geotech. Eng.*, **9**(4), 638-647. https://doi.org/10.1016/j.jrmge.2017.01.004.

Skinner, R.I., Tyler, R.G., Heine, A.J. and Robinson, W.H. (1980), "Hysteretic dampers for the protection of structures from earthquakes", *Bulletin Of The New Zealand National Society For Earthquake Engineering*, **13**(1), 22-36.

Stratan, A., Zub, C. and Dubina, D. (2020), "Prequalification of a set of buckling restrained braces: Part I - experimental tests", *Steel Compos. Struct.*, **34**(4), 547-559. https://doi.org/10.12989/scs.2020.34.4.547.

Takeuchi, T., Ida, M., Yamada, S. and Suzuki, K. (2008), "Estimation of Cumulative Deformation Capacity of Buckling

Restrained Braces", *J. Struct. Eng.*, **134**(5), 822-831. https://doi.org/10.1061/(ASCE)0733-9445(2008)134:5(822).

Toghroli, A., Mehrabi, P., Shariati, M., Trung, N.T., Jahandari, S. and Rasekh, H. (2020), "Evaluating the use of recycled concrete aggregate and pozzolanic additives in fiber-reinforced pervious concrete with industrial and recycled fibers", *Constr. Build. Mater.*, **252**, 118997. https://doi.org/10.1016/j.conbuildmat.2020.118997.

Tremblay, R., Bolduc, P., Neville, R. and DeVall, R. (2006), "Seismic testing and performance of buckling-restrained bracing systems", *Can. J. Civil Eng.*, **33**(2), 183-198.

Tremblay, R., Bolduc, P., Neville, R. and DeVall, R. (2006), "Seismic testing and performance of buckling restrained bracing systems", *Can. J. Civil Eng.*, **33**, 183-198. https://doi.org/10.1139/l05-103.

Tremblay, R., Poncet, L., Bolduc, P., Neville, R. and DeVall, R. (2004), "Testing and design of buckling restrained braces for Canadian application", *Proceedings of the 13th World Conference on Earthquake Engineering*, Vancouver, B.C., Canada, August 1-6.

Tsai, K.C., Chen, H.W., Hong, C.P. and Su, Y.F. (1993), "Design of steel triangular plate energy absorbers for seismic-resistant construction", *Earthq. Spectra*, **9**(3), 505-528. https://doi.org/10.1193/1.1585727.

Tsai, K.C. and Weng, C.H. (2002), *Experimental responses of double-tube unbonded brace elements and connections*, National Taiwan University.

Uriz, P. (2008), *Toward earthquake-resistant design of concentrically braced steel-frame structures*, Berkeley, Calif.: Pacific Earthquake Engineering Research Center.

Usefi, N., Ronagh, H. and Mohammadi, M. (2018), "Finite element analysis of hybrid cold-formed steel shear wall panels", in *ASEA-SEC04*, Queensland, Australia.

Usefi, N., Ronagh, H. and Sharafi, P. (2020), "Lateral performance of a new hybrid CFS shear wall panel for mid-rise construction", *J. Constr. Steel Res.*, **168**, 106000. https://doi.org/10.1016/j.jcsr.2020.106000.

Watanabe, A., Hitomi, Y., Saeki, E., Wada, A. and Fujimoto, M. (1988), "Properties of brace encased in buckling-restraining concrete and steel tube", *Proceedings of the 9th world conference on earthquake engineering*, Tokyo-Kyoto, Japan.

Xie, Q. (2005), "State of the art of buckling-restrained braces in Asia", *J. Constr. Steel Res.*, **61**(6), 727-748.

Xu, L., Fan, X., Lu, D. and Li, Z. (2016), "Hysteretic behavior studies of self-centering energy dissipation bracing system", *Steel Compos. Struct.*, **20(6)**, 1205-1219. http://dx.doi.org/10.12989/scs.2016.20.6.1205

.Yoshino, T. and Karino, Y. (1971), "Experimental study on shear wall with braces: Part 2. Summaries of technical papers of annual meeting", *Architect. Inst. Japan, Struct. Eng. Section*, **11**, 403-404.

Zub, C., Stratan, A. and Dubina, D. (2020), "Prequalification of a set of buckling restrained braces: Part II - numerical simulations", *Steel Compos. Struct.*, **34**(4), 561-580. https://doi.org/10.12989/scs.2020.34.4.561.

BU